NASA TECHNICAL NOTE

NASA TN D-2882

IONOSPHERE TOPSIDE SOUNDER STUDIES

I—THE REDUCTION OF ALOUETTE I IONOGRAMS TO ELECTRON DENSITY PROFILES

by J. O. Thomas, B. R. Briggs, L. Colin,
M. J. Rycroft, and Margaret Covert

Ames Research Center
Moffett Field, Calif.

NATIONAL AERONAUTICS AND SPACE ADMINISTRATION • WASHINGTON, D. C. • JULY 1965

NASA TN D-2882

IONOSPHERE TOPSIDE SOUNDER STUDIES

I - THE REDUCTION OF ALOUETTE I IONOGRAMS TO ELECTRON DENSITY PROFILES

By J. O. Thomas, B. R. Briggs, L. Colin,
M. J. Rycroft, and Margaret Covert

Ames Research Center
Moffett Field, Calif.

NATIONAL AERONAUTICS AND SPACE ADMINISTRATION

For sale by the Clearinghouse for Federal Scientific and Technical Information
Springfield, Virginia 22151 – Price $2.00

TABLE OF CONTENTS

IONOSPHERE TOPSIDE SOUNDER STUDIES, I:

THE REDUCTION OF ALOUETTE I IONOGRAMS

TO ELECTRON DENSITY PROFILES

By J. O. Thomas, B. R. Briggs, L. Colin,
M. J. Rycroft, and Margaret Covert
Ames Research Center

SUMMARY

In radar soundings of the topside of the ionosphere, an ionosonde in a vehicle immersed in the plasma above the peak of the F2 layer measures, as a function of frequency, f, the virtual depth, h', below the vehicle, at which radio waves are reflected from the topside of the ionosphere. In this report, a number of mathematical procedures and digital computer programs for converting the observed topside h'(f) curves into electron density profiles are described.

INTRODUCTION

The experiments carried on board the Canadian satellite Alouette have been described in reference 1 and by Warren (refs. 2 and 3). The first results have been presented in a series of papers in the Canadian Journal of Physics (refs. 4 to 9). Details concerning the construction, operation and orbit characteristics of the satellite can be found in the references quoted above.

In the topside sounder experiment (see section entitled "The Basic Problem") the virtual depths of reflection below the satellite, h', of radio pulses vertically incident on the topside ionosphere are measured as a function of frequency, f. The resulting topside h'(f) data, when displayed on photographic paper or film, are known as ionograms. These ionograms contain information about the distribution of electron density with height in the lower exosphere, a detailed knowledge of which is important for the physics of the ionosphere. The derivation of the electron density distribution as a function of height (N(h) profiles) from the ionogram is, however, a complicated procedure best carried out by a digital computer program.

This report presents information concerning such calculations which have been programmed at the NASA Ames Research Center for an IBM 7094 digital computer. These programs, in conjunction with a supplementary program described in a companion paper (ref. 10), are particularly suitable for the routine reduction of Alouette I ionograms to topside N(h) profiles and form an extension of work described recently by Thomas and Sader (refs. 11 and 12), Thomas, Long and Westover (ref. 13) and Thomas and Westover (ref. 14).

The basic problem is first described. The relevant calculations and procedures used for testing the computations together with details concerning the operational procedures to be employed for converting an ionogram to an electron density profile are subsequently presented.

In the last section the advantages and disadvantages of each technique are discussed, and test and sample cases presented in graphic and tabular form. The tabulated $h'(f)$ curves and corresponding $N(h)$ profiles computed both for model and real ionospheres can be used for comparison purposes and for testing newly developed programs.

Appendixes are included which prescribe standardized ionogram scaling or digitizing procedures and describe in detail the existing $h'(f)$ input and $N(h)$ output formats.

The authors wish to acknowledge gratefully the courtesy of scientists of the Canadian Defence Research Telecommunications Establishment, Ottawa, Canada, particularly Dr. J. H. Chapman and Dr. G. L. Nelms who made a number of top-side ionograms available to the authors in the early stages of development of this work. They wish also to thank the staff of the Radioscience Laboratory, Stanford University, for recording ionograms.

NOMENCLATURE

The symbols listed below define physical quantities. Symbols introduced in mathematical derivations are defined as needed in the text and are not listed here.

c	speed of light
f	frequency of a radio pulse
f'	defined as $\sqrt{f_x^2 - f_x f_H}$ for $f_x > f_H$
f_H	electron gyrofrequency
f_N	plasma frequency
F	total magnitude of the geomagnetic field
G_o	defined as $\mu_o' \sqrt{1 - (f_N/f_i)^2}$
G_x	defined as $\mu_x' \sqrt{1 - (f_N/f_i')^2}$
h	real height above the surface of the earth

h'_i virtual depth below the satellite

H' group retardation

I magnetic dip angle

N electron density

t time

u group velocity

Δh real depth measured positively downward from the vehicle

μ'_o group refractive index of the Ordinary ray

μ'_x group refractive index of the Extraordinary ray

Subscripts

i discrete value

o quantity related to the Ordinary trace

x quantity related to the Extraordinary trace

v quantity measured at the position of the vehicle

THE BASIC PROBLEM

In ionospheric variable frequency vertical incidence radio-pulse soundings from the ground or from satellite-borne radars, the time delay t between the emission of a radar pulse and the reception of an echo after its round trip from the transmitter to the point of reflection and back is measured. The virtual height of reflection above the ground, or, for a topside sounder, the virtual depth of reflection below the satellite h', is defined by

$$h' = \frac{1}{2} ct \tag{1}$$

where c is the velocity of light. The virtual height or depth thus corresponds to the distance which the radio pulse would have covered if it had everywhere along its path traveled with the velocity of light.

In a plasma, the real speed of the pulse is given by the group velocity u so that

$$u = \frac{dh}{dt} \tag{2}$$

where h is the real distance traveled by the pulse. Thus the total time of flight of the pulse and echo is given by

$$t = 2 \int_o^h \frac{dh}{u} \tag{3}$$

so that

$$h' = c \int_o^h \frac{dh}{u} \tag{4}$$

The group refractive index μ' is defined as c/u and can be calculated for the Ordinary and Extraordinary rays from the Appleton-Hartree magneto-ionic equation.

Hence, showing the functional dependencies of the quantities concerned we may write, neglecting the effect of collisions and measuring h and h' from the ground,

$$h'(f) = \int_o^{h(N)} \mu'(f,N,I,F)dh \tag{5}$$

where

f frequency of radio pulse

N electron density (a function of height)

I magnetic dip angle

F total magnitude of the earth's magnetic field

Equation (5) may also be related to the plasma frequency, f_N, and electron gyrofrequency, f_H, by the relations

$$N \simeq 1.2388 \times 10^4 \, f_N^2 \quad \text{and} \quad f_H \simeq 2.7994 \, F$$

with f_N and f_H given in Mc/s, N in electrons per cc and F in gauss. Thus,

$$h'(f) = \int_o^{h(f_N)} \mu'(f,f_N,I,f_H)dh \tag{6}$$

This is the basic equation relating the observed $h'(f)$ data to the $N(h)$ profile. In practice it is necessary to invert equation (6) so that $h(f_N)$ can be determined given $h'(f)$. In order to do this, it is convenient to transform (6) so that for the measurements of the Ordinary ray

$$h'_o(f_i) = \int_o^{f_i} \mu'_o \left(\frac{dh}{df_N}\right) df_N \tag{7a}$$

The subscript i indicates a value of frequency corresponding to a particular value, h_i, of real height and to a particular value, h'_i, of the virtual height measured on an ionogram. The upper limit of integration in equation (7a) is the plasma frequency in the region where the Ordinary ray of frequency f_i is reflected. For the Extraordinary ray

$$h'_x(f_{xi}) = \int_o^{f'_i} \mu'_x \left(\frac{dh}{df_N}\right) df_N \tag{7b}$$

with

$$f'^2_i = f^2_{xi} - f_{xi}f_{Hi} \qquad (f_{xi} > f_{Hi}) \tag{8}$$

the subscript x being included to indicate that the frequency is now measured on the Extraordinary trace.

A particular frequency of f_{xi}, equal to f_{xb} say measured on the Extraordinary trace, is reflected from the same real height as an Ordinary ray of frequency f_a, say, if, and only if,

$$f'^2_b = f^2_{xb} - f_{xb}f_{Hb} = f_a^2 = f_N^2$$

The frequencies f_a and f_{xb} are then known as "corresponding" frequencies.

In general, one can write (see eq. (6))

$$h'(f) = \int_o^{\varphi(f_N)} \mu'(f, f_N, I, f_H) \left(\frac{dh}{d\varphi}\right) d\varphi \tag{9}$$

where φ is some single valued function of f_N, and f_H is the gyrofrequency for electrons. Equations (7a) and (7b) obviously correspond to the case $\varphi(f_N) = f_N$.

It should be noted that dh/df_N must remain finite over the interval concerned so that for the inversion of the $h'(f)$ curve it is required that $h(f_N)$ or, generally, $h(\varphi)$ be monotonic.

Equations (7a) and (7b) apply for ground-based soundings. They may be rewritten, with slight notational changes, for application to topside ionograms, as follows:

$$h'_o(f_i) = \int_{f_v}^{f_i} \mu'_o \left(\frac{d\ \Delta h}{df_N}\right) df_N \qquad (10)$$

$$h'_x(f_{xi}) = \int_{f'_v}^{f'_i} \mu'_x \left(\frac{d\ \Delta h}{df_N}\right) df_N \qquad (11)$$

The subscript v in the lower limits of these two integrals indicates that the plasma frequency is that at the position of the vehicle, and Δh is used here for the real depth of reflection below the satellite. Equation (9) may be altered similarly giving, for the Ordinary ray, for example

$$h'_o(f) = \int_{\varphi(f_v)}^{\varphi(f_N)} \mu'_o(f, f_N, I, f_H) \left(\frac{d\ \Delta h}{d\varphi}\right) d\varphi \qquad (12)$$

From equation (10), (11) or (12) it is possible to deduce $\Delta h(f_N)$ from the observed $h'(f)$ variation recorded on the topside ionogram. This may subsequently be converted into an electron density profile giving N as a function of h, the height above the ground by means of the relation $\Delta h = h_v - h$ where h_v is the height of the satellite.

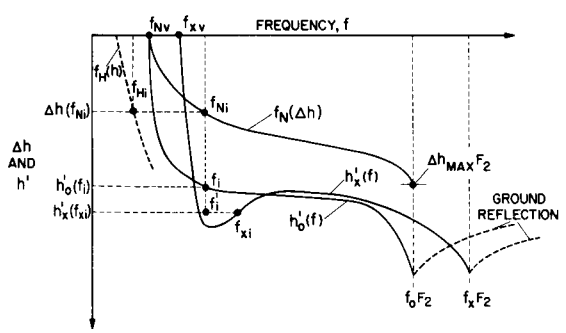

Fig. 1.- Schematic diagram of a typical topside electron density profile $[f_n(\Delta h)]$ and its associated Extraordinary $[h'_x(f)]$ and Ordinary $[h'_o(f)]$ ionogram traces. In this diagram f_{xi} has been chosen as the "corresponding frequency to f_i (see text).

In procedures described in the subsequent pages for the inversion of equations (10), (11) and (12) it is assumed that the plasma frequency f_v or f'_v at the vehicle is known, as are also the quantities I, f_H and h_v. Techniques for determining these four parameters are described in reference 10. It should be noted that in computing f'_i or f'_v from equation (8) the appropriate value f_{Hi} or f_{Hv} of the height-dependent gyrofrequency should be used.

Figure 1 illustrates schematically a typical topside profile with associated Ordinary and Extraordinary ray traces.

DIGITAL COMPUTER PROGRAMS FOR THE REDUCTION OF TOPSIDE IONOGRAMS TO ELECTRON DENSITY PROFILES

General Remarks

Several programs are available at the NASA Ames Research Center for reducing topside ionogram data. The techniques used are noted below and are directly based on, or are simple developments of, analytical procedures already extensively described in the scientific literature. The appropriate relevant references are given in table I for each technique.

1. Single polynomial method
2. Overlapping polynomial method
3. Lamination method
4. Contiguous parabola method

The input data include the dip angle at the vehicle I_V, the gyrofrequency at the position of the satellite, f_{HV}, and a number of pairs of frequency and virtual-depth data as read from an ionogram according to the reading or scaling procedure described in appendix A. Identification and control information is also read in. The input data are punched onto cards, in a single format which can be used for all the programs currently available. The punched card input formats are described in detail in appendix B.

The basic output for a single ionogram includes all of the input quantities, and the calculated real depth and electron density. Options are available in the overlapping polynomial program to print interpolated summary tables of electron density and scale height, H, as functions of real depth at 50-km intervals for a series of ionograms. The scale height H is approximated by $\left|N/(\Delta N/\Delta h)\right|$. Details of output formats for the several programs, as well as computer time estimates, are given in appendix C.

The Single Polynomial Method

The topside single polynomial program is essentially identical to that described briefly by Thomas, Long and Westover (ref.13) and in more detail in a report by Thomas and Westover (ref. 14). Basically the program consists of a simple development of the single polynomial technique (for references see table I) proposed by Titheridge (ref. 15) for the reduction of bottomside ionograms. The modification outlined briefly below allows for the two conditions appropriate to the topside case, namely, that both N and dN/dh are finite at $\Delta h = 0$.

It is assumed that the N(h) curve (or part of the N(h)) curve can be approximated by the polynomial

$$\Delta h = \sum_{j=1}^{n} \alpha_j (f_N - f_{Nv})^j \tag{13}$$

where f_{Nv} is the plasma frequency at the vehicle and n is the number of points through which the polynomial is to be fitted. Details are omitted here, but it is shown in the references noted above that Δh can be determined by solution of the matrix equation

$$[\Delta h] = [A][B^{-1}][h'] \tag{14}$$

The elements of [A] are

$$a_{ij} = (f_i - f_{Nv})^j \tag{15}$$

For the Ordinary ray the elements of [B] are

$$b_{ij} = j \int_{f_{Nv}}^{f_i} \mu_o'(f_N - f_{Nv})^{j-1} \, df_N \tag{16}$$

Equation (16) may be written in the form

$$b_{ij} = jf_i \int_{\sin^{-1}(f_{Nv}/f_i)}^{\pi/2} G_o(f_i \sin\theta - f_{Nv})^{j-1} \, d\theta \tag{17}$$

where the transformation $f_N = f_i \sin\theta$ has been made, and where μ_o' has been replaced by the function $G_o \Big/ \sqrt{1 - (f_N^2/f_i^2)}$.

The above equations apply for the Extraordinary trace if f_i, μ_o' and G_o are replaced by f_i', μ_x' and G_x, respectively, where

$$f_i'^2 = f_{xi}^2 - f_{xi} f_{Hv}$$

and

$$\mu_x' = \frac{G_x'}{\sqrt{1 - (f_N^2/f_i'^2)}}$$

μ_o' and μ_x' are related to the frequency of the exploring radio wave, the electron density in the plasma and the strength and direction of the earth's field through the classical Appleton-Hartree magneto-ionic theory. Throughout the work described here, the calculation of the group refractive indexes (and of G_o and G_x) were made using the Appleton-Hartree equations in the formulation given by Becker (ref. 16). The relevant formulas are summarized in appendix D.

The electron density for each Δh_i is computed from

$$\left.\begin{aligned} N_i &= 1.2388\times10^4\, f_i^2 \text{(Ordinary ray)} \\ N_i &= 1.2388\times10^4\, f_i'^2 \text{(Extraordinary ray)} \end{aligned}\right\} \qquad (18)$$

The use of the single polynomial procedure is limited to cases where the N(h) profile is monotonic and the h'(f) curve contains no sharp "cusps."

The Overlapping Polynomial Method

The overlapping polynomial procedure described here is based on the work of Titheridge (ref. 15) who has applied this technique in the reduction of ground-based ionograms. Whereas the single-polynomial method cannot be used for reducing ionograms having cusps and other sharp irregularities, the overlapping polynomial method is quite generally applicable.

Instead of the entire N(h) profile being represented by a single polynomial, a number of polynomials are used over a series of small frequency ranges. Thus, when the real depth is calculated at any frequency, a polynomial to represent the exact shape near this frequency only is required, and virtual depths outside the particular range are not used. The polynomial is chosen to give the correct virtual depths at frequencies just above and below as well as at the frequency under consideration. The polynomial is also joined to an already determined part of the curve, and so a smooth continuation of the real depth curve with the correct gradient is assured.

In order to illustrate this, suppose that real depths have been determined at frequencies $f_1, f_2, \ldots, f_{i-1}$, and that it is desired to compute the real depth corresponding to frequency f_i (see fig. 2). A fourth-degree polynomial

$$\Delta h = \sum_{j=0}^{4} \alpha_j f_N{}^j \qquad (19)$$

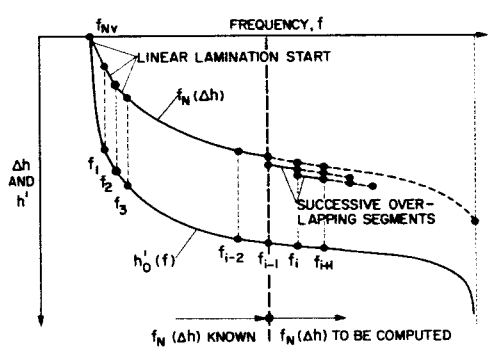

Fig. 2.- Schematic diagram illustrating the step by step and overlapping procedures by which a profile is deduced from Ordinary ray ionogram data by the overlapping polynomial technique.

will be found which smoothly connects the point at f_i on the $f_N(\Delta h)$ curve to the points at f_{i-1} and f_{i-2}, and such that the correct values for h' are maintained at f_{i-1} and also at f_{i+1}. The constants α_0, α_1, α_2, α_3 and α_4 are to be computed, following which Δh_i is calculated by substitution of f_i for f_N in equation (19). The five equations to be solved for the α's are

$$\left.\begin{aligned} \Delta h_m &= \sum_{j=0}^{4} \alpha_j f_m{}^j \ , \qquad \text{for } m = i-2 \text{ and } i-1 \\ H'_{m,i-2} &= \sum_{j=1}^{4} j\alpha_j \int_{f_{i-2}}^{f_m} \mu'_o(f_m,f_N) f_N^{j-1}\, df_N \ , \qquad \text{for } m = i-1, i, i+1 \end{aligned}\right\} \tag{20}$$

The group retardations $H'_{m,i-2}$ are given by the integral

$$H'_{m,i-2} = \int_{\Delta h_{i-2}}^{\Delta h_m} \mu'_o(f_m,f_N)\, d(\Delta h)$$

or

$$H'_{m,i-2} = -\int_{f_v}^{f_{i-2}} \mu'_o(f_m,f_N)\left(\frac{d\,\Delta h}{df_N}\right) df_N + h'_m \tag{21}$$

The numerical treatment of this integral, as well as those in equations (20), will be discussed later.

Special consideration is needed for the last point (point n), since point n + 1 does not exist. A third-degree polynomial

$$\Delta h = \sum_{j=0}^{3} \alpha_j f_N{}^j \tag{22}$$

is used, and the four equations to be solved for α_0, α_1, α_2 and α_3 are

$$\left.\begin{aligned} \Delta h_m &= \sum_{j=0}^{3} \alpha_j f_m{}^j , \qquad \text{for } m = n-2 \text{ and } n-1 \\ H'_{m,n-2} &= \sum_{j=1}^{3} j\alpha_j \int_{f_{n-2}}^{f_m} \mu'_o(f_m, f_N) f_N^{j-1}\, df_N , \qquad \text{for } m = n-1 \text{ and } n \end{aligned}\right\} \quad (23)$$

The group retardations H' are again defined as in equation (21).

The required two starting values for the overlapping polynomial procedure are determined by use of a lamination method (see following section and table I) suitably modified for the topside application.

The evaluation of the integrals in equations (20), (21) and (23) is facilitated by the introduction of the transformation $f_N = f_m \sin\theta$ ($f_N = f'_m \sin\theta$ in the case of the Extraordinary trace). The integrals in equations (20) and (23) become

$$j \int_{f_{i-2}}^{f_m} \mu'_o f_N^{j-1}\, df_N = j f_m \int_{\sin^{-1}(f_{i-2}/f_m)}^{\pi/2} G_o(f_m \sin\theta)^{j-1}\, d\theta \quad (24)$$

The calculation of μ'_o by use of the function G_o is discussed in appendix D. The integral in equation (21) is handled in a similar manner. First, however, it is necessary to evaluate the derivative $d(\Delta h/df_N)$ in the frequency range of f_{Nv} to f_{i-2}. Since Δh has already been calculated in this range, this can be done by means of a simple linear approximation between given frequency values. Equation (21) then becomes

$$H'_{m,i-2} = h'_m - \sum_{k=1}^{i-2} \left[\left(\frac{\Delta h_k - \Delta h_{k-1}}{f_k - f_{k-1}} \right) \int_{f_{k-1}}^{f_k} \mu'_o(f_m, f_N)\, df_N \right]$$

for $m = i-1$, i, and $i+1$

or

$$H'_{m,i-2} = h'_m - \sum_{k=1}^{i-2} \left[\left(\frac{\Delta h_k - \Delta h_{k-1}}{f_k - f_{k-1}} \right) f_m \int_{\sin^{-1}(f_{k-1}/f_m)}^{\sin^{-1}(f_k/f_m)} G_o\, d\theta \right] \quad (25)$$

(Note that $f_o = f_{Nv}$ and $\Delta h_o = 0.$) Equations (19) through (25) apply for the Extraordinary trace if f_i, μ_o' and G_o are replaced by f_i', μ_x' and G_x, respectively (see appendix D).

In the case of Extraordinary trace data, a correction is made, following the calculation of the real depths, to adjust for the fact that a constant gyrofrequency (namely, f_{Hv}) has been used throughout. This correction consists in approximating f_{Hi} at each value of Δh_i(km) by the inverse cube relation

$$f_{Hi} = f_{Hv}\left(\frac{7370.0}{7370.0 - \Delta h_i}\right)^3 \tag{26}$$

and then recalculating f_i' using the relation

$$f_i' = \sqrt{f_{xi}^2 - f_{xi}f_{Hi}} \tag{27}$$

The electron density is then computed by the use of the formulas

$$\left.\begin{aligned} N_i &= 1.2388\times10^4\ f_i^2, \text{ Ordinary trace} \\ &= 1.2388\times10^4\ f_i'^2, \text{ Extraordinary trace} \end{aligned}\right\} \tag{28}$$

As noted earlier, the overlapping polynomial process is started by use of the linear lamination method. The program is arranged so that any number of points and, in fact, the entire profile, may be calculated by the lamination method. In practice, a three-point start is adequate for the overlapping polynomial program. It is occasionally of interest, however, to use the lamination method throughout.

The Linear Lamination Method

The linear lamination technique for the calculation of N(h) profiles from h'(f) curves (refs. 17 and 18) is based on the inversion of the integral equation (9) with $\varphi = f_N$ so that, for example, for the Ordinary ray

$$h_j' = \int_{f_v}^{f_i} \mu_o'\left(\frac{d\ \Delta h}{df_N}\right) df_N \tag{29}$$

Here $d\,\Delta h/df_N$ is assumed constant over each lamination. An outline of the method as applied to the topside case is given here, based on a simple modification to the procedure for bottomside ionograms described by Thomas and Vickers (ref. 19). It may be noted that certain notation, namely the indexing of quantities, is in agreement with that used by Thomas and Vickers and is slightly different from that in the foregoing sections.

The true and virtual heights are assumed to be related by the following set of equations:

$$\left.\begin{aligned} h'_o &= A_{oo}\,\Delta h_o = 0 \\ h'_1 &= A_{1o}\,\Delta h_o + A_{11}\,\Delta h_1 \\ h'_2 &= A_{2o}\,\Delta h_o + A_{21}\,\Delta h_1 + A_{22}\,\Delta h_2 \\ &\vdots \\ h'_n &= A_{no}\,\Delta h_o + A_{n1}\,\Delta h_1 + \cdots + A_{nn}\,\Delta h_n \\ &\vdots \end{aligned}\right\} \tag{30}$$

Since $\Delta h_o = h'_o = 0$, as noted above, the first of equations (30) drops out, and terms multiplied by Δh_o in the subsequent equations are zero. The resulting set can be written as the matrix equation

$$[h'] = [A][\Delta h] \tag{31}$$

The equations represented by equation (31) solved one at a time, lead to

$$[\Delta h] = [B][h'] \tag{32}$$

which yields the desired values of $\Delta h(f_N)$ for the given $h'(f)$. In the above equation, the elements of [B] are

$$\left.\begin{aligned} B_{nn} &= \frac{1}{A_{nn}}\,, & m &= n \\ B_{nm} &= -\frac{A_{nm}}{A_{nn}}\,, & m &< n \\ B_{nm} &= 0\,, & m &> n \end{aligned}\right\} \tag{33}$$

The values for Δh_1, Δh_2, . . . can be found in succession by use of the relation

$$\Delta h_{n+1} = \sum_{m=1}^{n} (B_{n+1,m}\, \Delta h_m) + B_{n+1,n+1} h'_{n+1} \tag{34}$$

It is assumed in the lamination technique that $d\,\Delta h/df_N$ is constant between adjacent points, so that

$$\frac{d\,\Delta h}{df_N} = \frac{\Delta h_m - \Delta h_{m-1}}{f_m - f_{m-1}} = \text{const.} \tag{35}$$

Equation (29) then becomes

$$h'_n = \sum_{m=1}^{n} (\Delta h_m - \Delta h_{m-1}) M_{nm} \tag{36}$$

where

$$\left.\begin{aligned} M_{nm} &= \int_{f_{m-1}}^{f_m} \mu'_o \frac{df_N}{(f_m - f_{m-1})}\,, \qquad m \leq n \\ &= 0\,, \qquad m > n \end{aligned}\right\} \tag{37}$$

(In the case of M_{11}, $f_o \equiv f_{Nv}$.) Equation (36) may be written as the matrix equation

$$[h'] = [M][D][\Delta h] \tag{38}$$

where

$$[D] = \begin{bmatrix} 1 & 0 & 0 & 0 \ldots \\ -1 & 1 & 0 & 0 \ldots \\ 0 & -1 & 1 & 0 \ldots \\ 0 & 0 & -1 & 1 \ldots \\ \cdot & & & \\ \cdot & & & \\ \cdot & & & \end{bmatrix} \tag{39}$$

Now equation (38) is equivalent to equation (31) and

$$[A] = [M][D] \tag{40}$$

Thus, the elements of [A] can be determined from equation (40), following which the elements of [B] can be computed using equations (33). The real depths Δh_1, Δh_2, . . . are then readily calculated from equation (34).

It was pointed out in the previous section that the overlapping polynomial program employs the lamination method to obtain starting values. The entire computation may be carried out using the lamination technique if special control cards are used in this program (see appendix B).

The Contiguous Parabola Method

A second-order polynomial lamination technique for converting topside ionograms to N(h) profiles has been described by Doupnik (ref. 20). In principle, the method is similar to the overlapping polynomial technique except for two important differences: the polynomial is of second order (i.e., parabolic), and the laminations do not overlap but are contiguous. It is believed that either the overlapping polynomial or contiguous parabola programs can be applied to topside profiles with equivalent accuracies for the same number of scaled h'(f) points. Each can be used for a wider class of ionograms than can the single polynomial or lamination programs and each gives higher accuracy than the lamination technique for a given number of h'(f) data points.

For mathematical detail concerning the contiguous parabola program the reader is referred to the report by Doupnik (ref. 20) who has supplied Ames Research Center with a "parabolic in $\ln f_N$" digital computer program which has been modified to accept input data in the standard Ames format (appendix B). It should be noted that the series of parabolas open along the real height axis and hence do not represent "parabolic layers." Parabolas in f_N and in $\ln f_N$ can be used and each has certain advantages, as discussed by Doupnik (ref. 20). The output format for the contiguous parabola program is described in appendix C. Some tests of the accuracy of the method are included in the next section.

DISCUSSION OF RESULTS, SELECTED EXAMPLES

In this section, a description is given of tests made to determine the accuracy of the computations described in the previous section.

Examples are presented of a number of h'(f) curves used as input data to the digital computer. The corresponding N(h) profiles deduced using the different techniques described can then be compared and the relative accuracy of each technique assessed. Other factors affecting the suitability of a particular technique when applied to routine ionogram reduction are also reviewed briefly. An attempt is made to estimate the over-all accuracy which can be attained with scaling and reduction techniques that are sufficiently short to

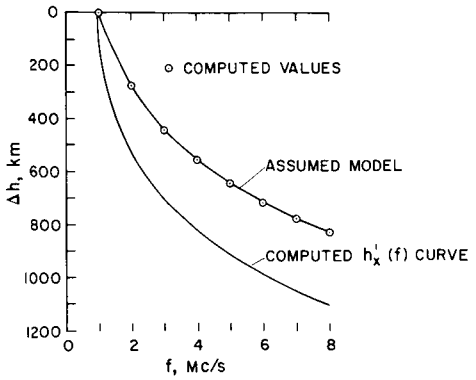

Fig. 3.- The accuracy to which an assumed exponential topside electron density profile can be recovered, from an analysis of the corresponding $h'_x(f)$ curve, by the single polynomial technique.

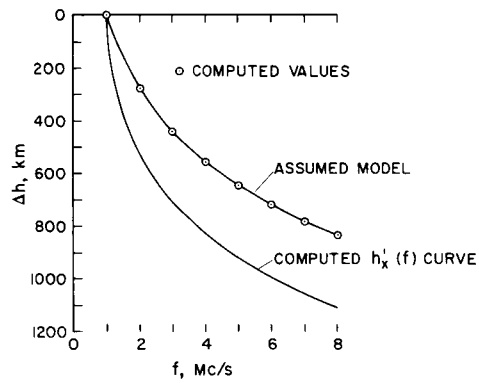

Fig. 4.- The accuracy to which an assumed exponential topside electron density profile can be recovered, from an analysis of the corresponding $h'_x(f)$ curve, by the contiguous parabola technique.

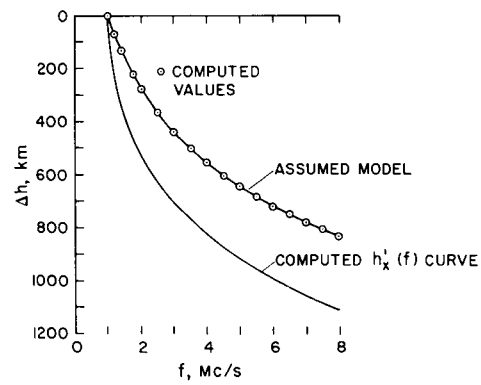

Fig. 5.- The accuracy to which an assumed exponential topside electron density profile can be recovered, from an analysis of the corresponding $h'_x(f)$ curve, by the overlapping polynomial technique.

enable large numbers of ionograms to be reduced to N(h) profiles in an economical and rapid manner.

In order to check the accuracy of the computations, two kinds of tests were devised. In the first of these (described below under the heading No-Field Case) a model ionosphere is assumed such that a simple analytical expression exists for the virtual depth as a function of frequency. This expression is used for computing the h'(f) curve to any desired accuracy. This provides a test ionogram which may be read into the digital computer as a data curve containing essentially zero scaling errors. The N(h) profile deduced by the different computer reduction techniques can then be compared with the exactly known starting N(h) model and hence the absolute accuracy of the computations can be assessed.

In the second kind of test, an actual topside ionogram is read and a table formed giving values of h' and corresponding values of f. The N(h) profiles deduced using the various reduction techniques together with the tabular values of h' and f are then compared. The errors in reading h' and f can be estimated by comparing the N(h) profile deduced from a number of independent readings of a given ionogram. Further details are given in the following paragraphs.

No-Field Case

When there is no magnetic field, it is possible to choose realistic analytic approximations to topside profiles which are amenable to exact closed-form solutions of equations (10), (11) and (12). One such topside model is an exponential decay of plasma density with real depth corresponding to the curve

$$\Delta h = 400 \ln f$$

and shown as the upper curve in figures 3, 4 and 5. The corresponding

$h'_x(f)$ curve is given by

$$h' = 400 \cosh^{-1} f$$

Corresponding values of $h'(f)$ are presented in the first two columns of table II and plotted as the lower curve in figures 3, 4 and 5.

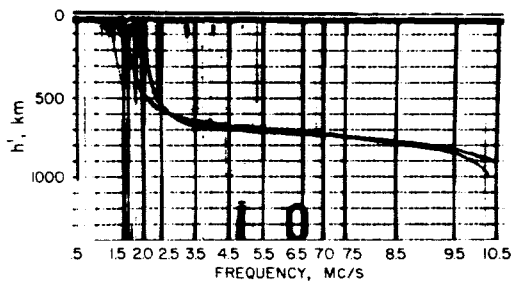

Fig. 6.- Typical equatorial Alouette topside ionogram used as standard test for reduction of Alouette N(h) data. The ionogram was recorded at Singapore on Alouette pass number 697 on November 19, 1962, at 0810 UT. The latitude and longitude of the subsatellite point was 11.6° S and 117.2° E, respectively. At this time the satellite was at an altitude of 1003.2 km, and the electron gyrofrequency at the vehicle was 0.81 Mc/s. Strong Ordinary and Extraordinary traces and a weak Z-trace are evident in addition to plasma and gyrofrequency resonances.

Values of h' and f computed from the above expression were read into the digital computer and the $N(h)$ profile deduced using the single polynomial, contiguous parabola, and overlapping polynomial techniques. The corresponding computed $f(\Delta h)$ points for each technique are shown as circles in figures 3, 4 and 5 from which it can be seen that the assumed profile is recovered to a high degree of accuracy. Table II shows the values of Δh computed with the overlapping polynomial technique (column 3) together with the exact values. It is seen that the $f(\Delta h)$ curve is recovered everywhere to better than ~1 km with a mean difference between the computed and exact $N(h)$ curves of less than 0.4 km.

Magnetic Field Included

When the magnetic field strength is finite, there is no analytic profile model available which is amenable to exact closed-form solution as above. Hence, it is not possible to check the absolute accuracy of a given reduction technique or associated computer program. However, the relative accuracies may be estimated by comparing the $N(h)$ profile deduced by each technique from a given set of $h'(f)$ points. For this purpose the NASA Topside Working Group has chosen a working ionogram taken from an actual Alouette I frame (fig. 6). Table III lists digitized values of $h'_o(f)$ and $h'_x(f)$, as scaled from figure 6 by one representative of the Topside Working Group. These values are to be used as standard inputs to the various reduction programs. The circles and squares in figure 7 are plots

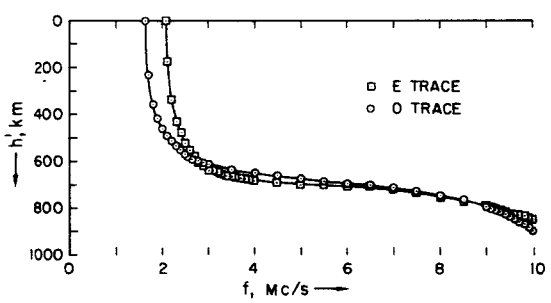

Fig. 7.- Plot of $h'_o(f)$ and $h'_x(f)$ for test ionogram of figure 6. See table III for values.

of these tabulated points; smooth lines join them. Each member organization of the Topside Working Group computed an N(h) profile using the data of table III. Different reduction techniques were employed and a smooth composite profile based on all the resulting N(h) data as drawn by the Topside Working Group is shown in figure 8 and tabulated in table IV.

The h'(f) data of table III were used as inputs to the Ames Research Center reduction programs. The resulting N(h) profiles, for the linear lamination, contiguous parabola and overlapping polynomial programs are shown in figures 9, 10 and 11, respectively. In each of these figures the squares

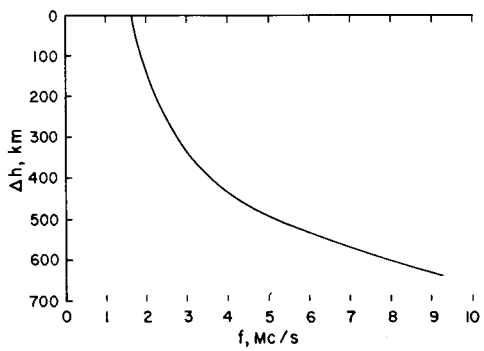

Fig. 8.- "Composite" Topside Working Group electron density profile resulting from reduction of the tabulated values of the test ionogram by at least eight different computer programs as provided by at least four different research groups. The graph is a "mean" curve through points having a typical scatter of ±1 to 2 km.

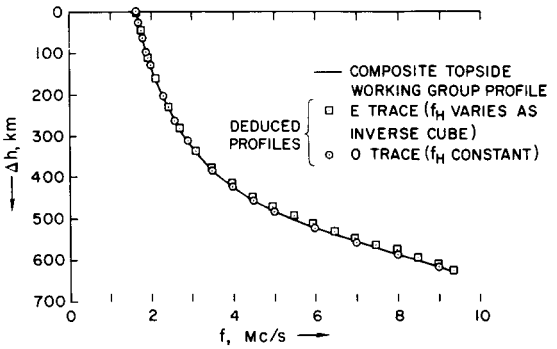

Fig. 9.- Test of NASA Ames Research Center technique for the reduction of h'(f) curves to N(h) profiles (lamination method - see table I). The input data were the values in table III. An inverse cube height variation is allowed for in the E trace analysis; constant f_H is assumed in the O trace analysis.

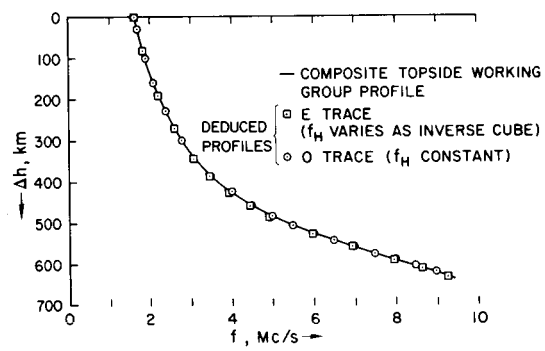

Fig. 10.- Test of NASA Ames Research Center techniques for the reduction of h'(f) curves to N(h) profiles (contiguous parabola technique - see table I). The input data were the values in table III. An inverse cube height variation is allowed for in the E trace analysis; constant f_H is assumed in the O trace analysis.

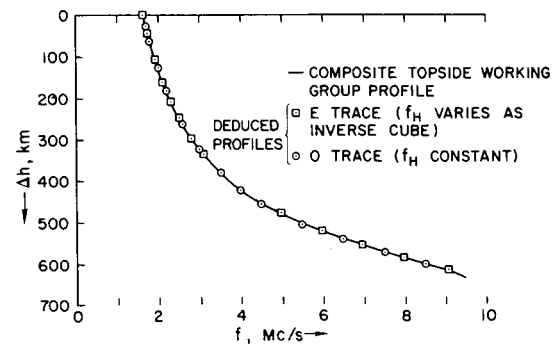

Fig. 11.- The accuracy with which an overlapping polynomial technique produces results comparable with the "composite" profile of figure 8 (continuous curve). The h'(f) values of table III were used as input data. An inverse cube height variation is allowed for in the E trace analysis; constant f_H is assumed in the O trace analysis.

represent the profile deduced from the tabulated Extraordinary trace data and the circles represent the profile deduced from the tabulated Ordinary trace data. The smooth curve is the Topside Working Group's composite profile of figure 8. In all cases, the deduced N(h) profile agrees well with the Topside Working Group's curve, with the contiguous parabola and overlapping polynomial techniques giving a more accurate profile than the linear lamination method. Numerical values of f_N and Δh deduced from the Extraordinary and Ordinary traces, using the overlapping polynomial program, are presented in table V.

Scaling Accuracies

The main errors in ionogram-profile reduction arise from inaccuracies in ionogram scaling. Since the basic problem concerns the rapid, but accurate, reduction of large quantities of topside ionograms electronic digitizing machines, rather than manual scaling techniques, have been primarily employed. The squares in figure 12 show the Extraordinary trace of the ionogram of figure 6 scaled using a Benson-Lehner OSCAR-F electronic digitizer. The smooth curve of figure 7, representing tabulations of the same trace by the Topside Working Group, is superimposed. It is clear that errors of ~10 km in h' can arise even when the curves are carefully, but fairly rapidly, scaled. Thus random variations of ~4 km are likely to occur in the N(h) profile as a result of scaling errors. Figure 13 compares the deduced profile using the digitized h'(f) data of figure 12 as inputs to the overlapping polynomial program (squares) with the profile deduced with the same program using the h'(f) data of table III as inputs (smooth curve).

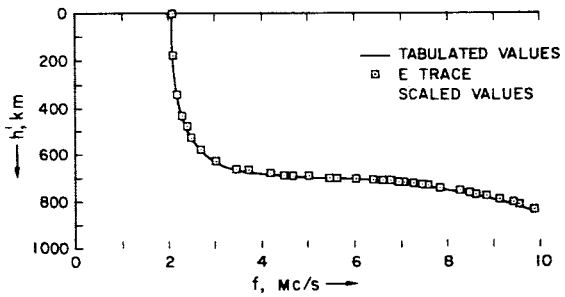

Fig. 12.- Comparison of ionogram scaling produced by two independent groups.

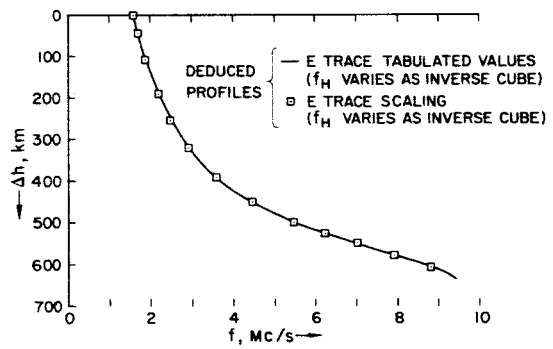

Fig. 13.- Two profiles computed from the test ionogram scaled by two independent groups by an overlapping polynomial program.

Variation of Magnetic Field Strength With Height

It is important to note, that, especially for the topside ionosphere, it is necessary in the computations to allow for the variation of the magnetic field strength with height, particularly for Extraordinary trace analysis.

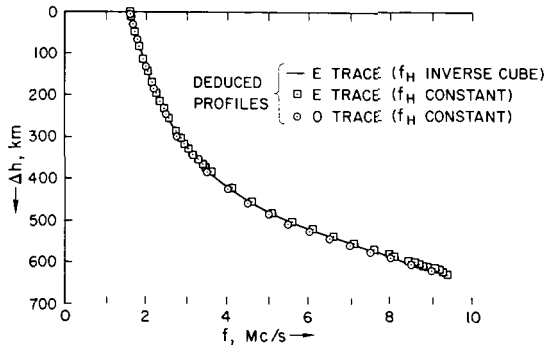

Fig. 14.- Improvement of the computed profile when a constant electron gyrofrequency is replaced by an inverse-cube variation of gyrofrequency with depth below the Alouette satellite. In both cases the reduction of the E trace was carried out by the overlapping polynomial method.

The circles in figure 14 represent the profile deduced from the Ordinary trace h'(f) test ionogram (table III) assuming a constant gyrofrequency with height. The squares represent the profile deduced from the Extraordinary trace (table III) again assuming a constant gyrofrequency. The smooth curve represents the profile deduced from the same Extraordinary trace when the gyrofrequency is assumed to increase with depth according to an inverse-cube law. Significantly better agreement between the profiles deduced from the Ordinary and Extraordinary trace data is achieved when the height-varying gyrofrequency is employed.

Nighttime Ionograms

The ionograms so far presented (figs. 3 and 6) have shapes typifying daytime conditions in the topside ionosphere. At night the appearance of the ionograms is different, the h'(f) curve showing a sharp cusp at low frequencies (fig. 15). Such rapid changes of h' with f can severely tax the ability of many computer techniques to produce a reasonable profile. Clearly, the single polynomial technique cannot be applied in such cases and neither can a lamination technique using large values of lamination depths. The contiguous parabola and overlapping polynomial techniques are adequate, however, and yield satisfactory results.

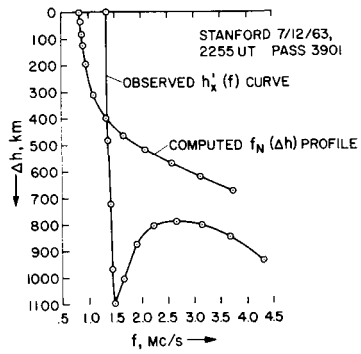

Fig. 15.- The manner in which an observed nighttime ionogram having a deep cusp in the E trace corresponds, when computed by the overlapping polynomial technique, to a smoothly varying $f_N(\Delta h)$ profile.

Figure 15 illustrates data from an actual Alouette nighttime ionogram. The profile deduced by the overlapping polynomial program is also shown in this figure and the associated numerical data are presented in table VI.

Ames Research Center
National Aeronautics and Space Administration
Moffett Field, Calif., Mar. 8, 1965

APPENDIX A

INSTRUCTIONS FOR SCALING TOPSIDE h'(f) RECORDS

INTRODUCTORY COMMENTS

The purpose of this appendix is to document detailed specifications for the scaling of Alouette I ionograms as data inputs to the N(h) digital computer programs described in the text. In general, these specifications apply for the contiguous parabola and overlapping polynomial programs. Minor additional considerations pertinent to the lamination and single polynomial programs are discussed at the conclusion of the appendix.

"Scaling" (or "reading") the curve is concerned with the representation of an Extraordinary and/or Ordinary topside ionogram by a finite number of pairs of h' and f values measured at suitable intervals along the trace. The accuracy and number of scaled points required for computing accurate profiles with the techniques available are considered. In practice, the Extraordinary trace is usually scaled since it is the more frequenty observed in its entirety. Hence, reference will be made to that trace only; scaling procedures for the Ordinary trace are similar.

FORMATS

As described elsewhere in this report, two distinct computer programs are utilized for converting ionograms to profiles. One program, described in reference 10 and designated here as the N_V program, requires, as ionogram data input, the frequency, f_{XV}, at which the Extraordinary trace has zero virtual depth, that is, $h'_X(f) = 0$, together with the time of occurrence of f_{XV} measured to ±0.5 second. The input ionogram data format for this program is shown in table VII. In addition to the time and f_{XV}, auxiliary data required are the pass number, date and telemetry station. Table VIII illustrates the positional data input format for the N_V program. This table contains the longitude, latitude and height of the satellite for the given pass and date at times 1 minute apart such that the time of f_{XV} given in table VII falls between these two times. Whether or not the satellite is in sunlight at the time stipulated is indicated by an asterisk or a blank in column 41; for convenience the planetary index of magnetic activity, K_p, at the time is also listed. All positional data, in the format of table VIII, is punched by hand from "world maps" defining the Alouette I orbit. Table IX illustrates the output format for this N_V program. Several, but not all, of the output parameters are required as inputs to the N(h) programs.

Tables X and XI (appendix B) show the identification card input format and parameter card input format for the N(h) programs. The parameters common to tables IX, X and XI are pass number, date, time, dip angle,

gyrofrequency at the vehicle, f_{Hv} and f_{xv}. It should be noted that the quantities dip angle and f_{Hv} may be entered in the N(h) input format only after the N_v program has been run. Table XII illustrates the frequency-virtual depth data input format which contains all h' and f pairs for a given ionogram excluding the f_{xv} value. The reader is referred to reference 10 and appendix B herein for further necessary detail on input card formats.

IONOGRAM QUALITY AND VARIABILITY

Figures 16 and 17 illustrate "good" Alouette ionograms inasmuch as the Extraordinary trace has no large gaps, is narrow in width ($\leq$ 0.1 Mc/s in thickness at small h' and $\leq$ 20 virtual km in thickness at greater h'), and has fairly sharp contrast. These ionograms are rather easily scaled. Figure 16, typical of daytime quiet conditions, shows h'_x to be a smooth, monotonically increasing, single-valued function of f_x. On the other hand, figure 17 is typical of nighttime quiet conditions where f_x is a multivalued function of h'_x due to the evident cusp (large group retardation) at frequencies only slightly higher than f_{xv}. Considerable care must be exercised in the scaling of the latter ionogram and additional h' and f pairs may be required for equivalent accuracy (see below). Figure 18 illustrates a "poor" ionogram typical of "spread" ionospheric conditions. Clearly, any attempt to scale the latter would lead

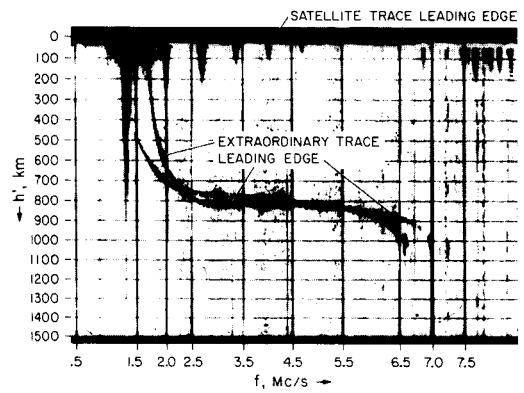

Fig. 16.- "Good" Alouette I ionogram illustrating typical daytime traces and the satellite trace.

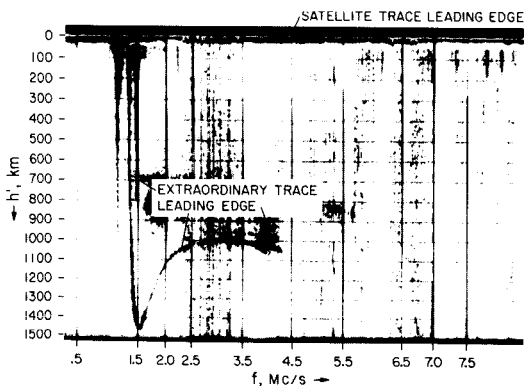

Fig. 17.- "Good" Alouette I ionogram illustrating typical nighttime Extraordinary and satellite traces.

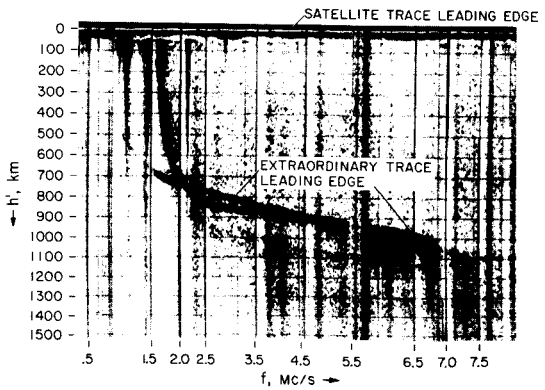

Fig. 18.- "Poor," but scalable, Alouette I ionogram illustrating typical disturbed ionospheric conditions.

only to a rough, first-order estimate of the real height. The ionograms which will be encountered in analyses of Alouette I records will range in quality and variability between those illustrated in figures 16 to 18. It should be noted from these figures that the satellite trace (equivalent to the ground pulse in ground-based sounders) provides the zero virtual depth measurement and must therefore also be of "good" quality.

GENERAL SCALING PROCEDURE

The basic requirement is to tabulate h'_X at a set of discrete frequencies for the Extraordinary trace from f_{XV} to f_XF_2 when the trace extends that far, or to the highest observable f_X. The Extraordinary trace is always the one that begins and ends farthest to the right on a given ionogram.

All h' and f points should be scaled at the leading edge of the trace (see figs. 16 to 18).

The zero-depth reference is always the leading, that is, top, edge of the satellite trace. The zero height marker should coincide with the leading edge of the satellite trace. Frequency calibration is afforded by the frequency markers. Linear interpolation between height markers and frequency markers can be used.

In general, scaling should only be attempted, and will only be reliable, when the leading edge is fairly well defined and when no large gaps exist in the trace (see figs. 16 and 17). Ionograms with gaps of less than 0.5 Mc/s, or even in some cases up to 1 Mc/s, may be scaled by simply reading a smoothly drawn curve through the gap bearing in mind the shape of the trace on similar days or on other ionograms within the pass.

When the h'(f) trace shows signs of severe scattering or masking by resonances, spurious responses, spread F, overlapping of Ordinary and Extraordinary traces, etc., it may not be possible to scale a given ionogram. If the masking is localized, particularly near f_XF_2, it may still be worthwhile to scale the ionogram by drawing a smooth curve across the locally masked area bearing in mind the shape of the trace on similar days or on other ionograms within the pass.

From an ionospheric physics viewpoint, very interesting effects are often prevalent on ionograms recorded during disturbed, rather than quiet, conditions. Hence, with some sacrifice in reliability, it may be advantageous to scale certain types of spread ionograms. An example is given in figure 18. It should be noted that this ionogram has an easily identified Extraordinary trace but has considerably more spread than the corresponding trace of figures 16 and 17. The trace has a rather well-defined trailing edge from 0 down to about 800 virtual km and a comparatively well-defined leading edge thereafter. One can therefore construct a scalable trace by drawing a smooth curve, from 0 to 800 virtual km, vertically above the trailing edge by an amount roughly equivalent to the width of the satellite trace, approximately

20 virtual km in such a manner that it smoothly joins the leading edge at greater depths. Such data should be marked with a sign to indicate this special procedure has had to be used.

SPECIFIC SCALING DETAILS

There is no absolute criterion for the number and density of scaled points. It is necessary that a minimum number of scaled points, meeting the criteria below, be used. Overscaling decreases the number of ionograms which can be read, per unit time, with no increase in accuracy. A minimum of 8 to 10 points is usually needed, rarely more than 15 to 20.

For traces of the type shown in figure 16 the leading edge is scaled at about 0.05 to 0.1 Mc/s intervals for the first few points. The remainder of the curve is scaled at intervals of about 0.5 to 1 Mc/s. For an accurate N(h) profile, these remaining values should be very carefully scaled. A typical example is given in curve a of figure 19. A total of not more than 10 pairs of values of h' and f should be sufficient.

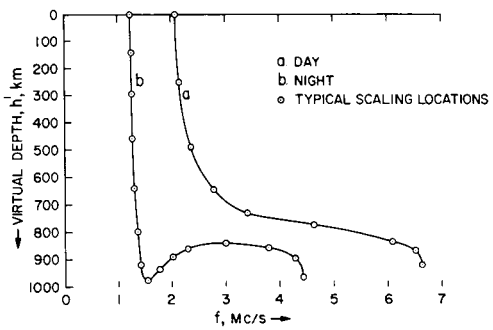

Fig. 19.- Typical daytime and nighttime sketched Extraordinary traces with suggested scaling locations.

For traces of the type shown in figure 17 it is necessary to scale in steps of between 0.01 and 0.05 Mc/s from f_{xv} down to and around the cusp, so that at least 7 or 8 points, including that at the cusp, are recorded in this interval. Following this, scaling is done in intervals of 0.2 to 1 Mc/s. Examples are given in curve b of figure 19 and in figure 15. A minimum of about 10 pairs of h' and f values are normally required for ionograms having "low" cusps with as many as 20 required for more extreme cases.

It is always necessary to ensure that successive frequency readings increase monotonically (assuming that the trace is scaled in the direction from f_{xv} to f_xF_2).

Irregularities with a scale of < 0.1 Mc/s or < 5 virtual km should be smoothed out unless otherwise advised (e.g., for special studies).

The input formats require h'_x to be rounded off to the nearest km and f_x to the nearest 0.01 Mc/s.

LAMINATION PROGRAM

In principle, it is possible to achieve equivalent accuracies with the lamination technique as compared with the contiguous parabola or overlapping

polynomial techniques. However, this requires a significant increase in the number of pairs of h' and f values (generally two to three times as many, Thomas and Vickers (ref. 19)) otherwise, the above scaling procedures apply.

SINGLE POLYNOMIAL PROGRAM

Because of the relatively large number of pairs of h' and f values required in the lamination program, the single polynomial and overlapping polynomial techniques (ref. 15) and contiguous parabola technique (Doupnik, ref. 20) were devised. Although the latter three techniques thus represent a significant improvement over the classical lamination approach, the single polynomial program suffers from the fact that a maximum of eight to nine pairs of h' and f values are useable (Thomas and Westover, ref. 14). Hence, this program is applicable to ionograms only of the class illustrated in figures 16 and 18. Ionograms showing cusps (as fig. 17) should never be reduced using the single polynomial program. Otherwise, the above scaling procedures apply.

APPENDIX B

INPUT FORMATS

The observed topside ionogram data (the h'(f) curves) are read into the digital computer on punched cards, the same format being used for each of the different programs. Special control cards are, however, required for selecting certain program options.

The standard input consists of three types of cards. These are an identification card, a card containing parameters, and a group of cards containing frequency and virtual height pairs, four pairs per card. Formats for these three types of input cards are shown in tables X, XI and XII.

It should be noted (table XI) that if the decimal point is included, the quantities I_V, f_{HV} and f_V (or f_{XV}) may be placed anywhere within the specified fields. The decimal point may be deleted, in which case it is understood to lie between the second and third positions from the right in the I_V field, and between the third and fourth positions from the right in the f_{HV} and f_V (or f_{XV}) fields.

The frequency and virtual depth data (table XII) may be punched with any format whatever, in the specified fields, if the decimal point is included. If the decimal point is deleted, it is understood to lie between the second and third positions from the right in the frequency fields, and to the right of the right-most position in the virtual depth fields. It should be pointed out that the first frequency and virtual depth pair on the first of a set of data cards is not the reading corresponding to zero virtual depth, but rather is the first reading at a finite virtual depth.

The single polynomial program and the contiguous parabola program will accept standard data as described above. A summary table of interpolated $N(\Delta h)$ values, which is routinely printed out by the single polynomial program, may be deleted if a "1" is punched in column 72 of the ionogram identification card. (This summary table is never prepared by the contiguous parabola program.)

The overlapping polynomial program is normally used with a three-point linear lamination method start, and interpolated tables of N versus Δh and scale height versus Δh are routinely saved. This procedure uses the standard data, as described in the foregoing paragraphs. If it is desired to use other than a three-point lamination start (or to compute the entire ionogram with the lamination method), or if it is desired to delete the two interpolated tables, then a modified version of the overlapping polynomial program is used, and a control card of the format described in table XIII is placed behind the data for each ionogram to be computed.

In all cases, a blank card is placed behind the last card in a run.

APPENDIX C

OUTPUT FORMATS

Detailed printouts are made for each ionogram. Examples are shown for an Extraordinary trace computation using the overlapping polynomial program and the contiguous parabola program in tables XIV and XV, respectively. It should be noted that pass number, date, time, dip angle I_V, gyrofrequency at the vehicle f_{Hv} and Extraordinary ray frequency at the vehicle f_{xv}, appear in the heading. Then columns of frequency, real and virtual depth and electron density are printed. The column headings for the Extraordinary ray "detailed output" are defined below.

Quantity	Overlapping polynomial	Contiguous parabola
h'	H PRIME	H
f_x	FX	F
f'	F PRIME	FN
Δh	DELTA H	DELTA H
N	ELECTRON DENSITY	DENSITY
Real height	- - -	Z
Gyrofrequency	- - -	FH

The two columns labelled A and B in table XV are intermediate quantities and have no physical meaning.

In the case of an Ordinary trace computation, the column for f_x (FX) does not appear, and f' (F PRIME) is replaced by f (F), in the overlapping polynomial program detailed output. Column headings are not changed in the contiguous parabola program; however, and the quantity f apears in both columns F and FN of the detailed printout.

A summary interpolated table of electron density versus real depth is available as output from the single polynomial and overlapping polynomial programs. An example is shown in table XVI. In addition, a summary interpolated table of scale height versus real depth is available as output from the overlapping polynomial program. The scale height is calculated by means of the formula

$$\text{Scale height} = \frac{2\Delta h_i N_i}{N_{i+1} - N_{i-1}}$$

where here, $\Delta h_i = \Delta h(N_i) - \Delta h(N_{i-1}) = \Delta h(N_{i+1}) - \Delta h(N_i) = 50$ km. An example of this output is shown in table XVII.

Approximate computing times have been determined on an IBM 7094 computer as follows:

(a) Single polynomial with $N(\Delta h)$ summary table, a 7-reading ionogram, 0.015 minute.

(b) Overlapping polynomial with $N(\Delta h)$ summary table, a 14-point ionogram, 0.040 minute.

(c) Contiguous parabola program, a 14-point ionogram, 0.080 minute.

APPENDIX D

CALCULATION OF GROUP REFRACTIVE INDICES

The Appleton-Hartree magneto-ionic equations in the formulation given by Becker (ref. 16) are used here to compute the group refractive indices μ_o' and μ_x'. The following definitions are made; first,

Ordinary ray	Extraordinary ray
$\mu_o' = G_o/t_o$	$\mu_x' = G_x/t_x$
$t_o^2 = 1 - \left(f_N^2/f_i^2\right)$	$t_x^2 = 1 - \left(f_N^2/f_i'^2\right)$
$y_o = f_H/f_i$	$y_x = f_H/f_j'$
$X_o = 1 - t_o^2$	$X_x = 1 - t_x^2$

Then, for the Ordinary ray,

$$G_o = \frac{t_o}{n_o}\left[1 + \frac{X_o \tan^2 I}{M^2}\left(\frac{1 + X_o}{\sqrt{1 + \gamma t_o^4}} - \frac{2}{1 + \sqrt{1 + \gamma t_o^4}}\right)\right] \tag{D1}$$

where

$$\left.\begin{aligned} \gamma &= \frac{4 \tan^2 I}{y_o^2 \cos^2 I}, \qquad M = 1 + t_o^2 \frac{2 \tan^2 I}{1 + \sqrt{1 + \gamma t_o^4}} \\ \left(\frac{n_o}{t_o}\right)^2 &= \frac{1 + \dfrac{2 \tan^2 I}{1 + \sqrt{1 + \gamma t_o^4}}}{1 + t_o^2 \dfrac{2 \tan^2 I}{1 + \sqrt{1 + \gamma t_o^4}}} \end{aligned}\right\} \tag{D2}$$

and for the Extraordinary ray,

$$G_X = \frac{t_X}{n_X}\left\{1 + \frac{X}{N^2}\left[1 + \frac{\beta}{2}\left(\frac{2\xi}{1 + \sqrt{1 + \alpha\xi}} - \frac{(1 + \xi)(1 + X)}{\sqrt{1 + \alpha\xi}}\right)\right]\right\} \tag{D3}$$

where

$$\left.\begin{aligned} &\alpha = \frac{4 \sin^2 I}{(1 + \sin^2 I)^2}, \qquad \beta = \frac{2 \sin^2 I}{1 + \sin^2 I} \\ &\xi = 2\Delta + \Delta^2 \\ &\Delta = t_X^2 \frac{1 - y}{y}, \qquad y = \frac{1}{2} y_X \left(\sqrt{4 + y_X^2} - y_X\right) \\ &X = (1 - y)X_X \\ &N = 1 - y + \Delta - \frac{\beta y \xi}{1 + \sqrt{1 + \alpha\xi}}, \qquad n_X^2 = y\xi \frac{1 - \dfrac{\beta}{1 + \sqrt{1 + \alpha\xi}}}{N} \end{aligned}\right\} \tag{D4}$$

Some limiting conditions are:

$$\left.\begin{aligned} &\lim_{t_O \to O} \frac{n_O}{t_O} = \frac{1}{\cos I} \\ &\lim_{t_O \to 1} G_O = 1 \end{aligned}\right\} \tag{D5}$$

$$\left.\begin{aligned} &\lim_{t_X \to O} \left(\frac{n_X}{t_X}\right)^2 = \frac{2}{\sin^2 I + 1} \\ &\lim_{t_X \to 1} G_X = 1 \end{aligned}\right\} \tag{D6}$$

REFERENCES

1. Canadian Defence Research Telecommunications Establishment: Alouette, Satellite 1962 Beta Alpha One. Canadian Defence Research Board, Ottawa, Canada, 1962.

2. Warren, E. S.: Sweep-Frequency Radio Soundings of the Topside of the Ionosphere. Can. J. Phys., vol. 40, no. 11, Nov. 1962, p. 1692.

3. Warren, E. S.: Some Preliminary Results of Sounding of the Topside of the Ionosphere By Radio Pulses From a Satellite. Nature, vol. 197, no. 4868, Feb. 16, 1963, pp. 636-9.

4. Warren, E. S.: Perturbation of the Local Electron Density by Alouette Satellite. Can. J. Phys., vol. 41, no. 1, Jan. 1963, pp. 188-9.

5. Lockwood, G. E. K.: Plasma and Cyclotron Spike Phenomena Observed in Top-Side Ionograms. Can. J. Phys., vol. 41, no. 1, Jan. 1963, pp. 190-4.

6. Petrie, L. E.: Top-Side Spread Echoes. Can. J. Phys., vol. 41, no. 1, Jan. 1963, p. 194.

7. Hagg, E. L.: A Preliminary Study of the Electron Density at 1000 Kilometers. Can. J. Phys., vol. 41, no. 1, Jan. 1963, pp. 195-8.

8. Muldrew, D. B.: The Relationship of F-Layer Critical Frequencies to the Intensity of the Outer Van Allen Belt. Can. J. Phys., vol. 41, no. 1, Jan. 1963, pp. 199-201.

9. Nelms, G. L.: Scale Heights of the Upper Ionosphere From Top-Side Soundings. Can. J. Phys., vol. 41, no. 1, Jan. 1963, pp. 202-6.

10. Thomas, J. O., Rycroft, M. J., Covert, Margaret, Briggs, B. R., and Colin, L.: Ionosphere Topside Sounder Studies, II: The Calculation of the Electron Density and the Magnetic Field Parameters at the Alouette I Orbit. NASA TN D-2921, 1965.

11. Thomas, J. O., and Sader, A. Y.: Alouette Topside Soundings Monitored at Stanford University. Tech. Rep. 6, NASA Grant NsG 30-60, Stanford Electronics Lab., Stanford Univ., 1963.

12. Thomas, J. O., and Sader, A. Y.: Electron Density at the Alouette Orbit. J. Geophys. Res., vol. 69, no. 21, Nov. 1964, pp. 4561-81.

13. Thomas, J. O., Long, A. R., and Westover, D.: The Calculation of Electron Density Profiles From Topside Sounder Records. J. Geophys. Res., vol. 68, no. 10, May 15, 1963, pp. 3237-42.

14. Thomas, J. O., and Westover, D. C.: The Calculation of Electron Density Profiles From Topside Ionograms Using a Digital Computer. Tech. Rep. 5, NASA Grant NsG 30-60, Stanford Electronics Lab., Stanford Univ., 1963.

15. Titheridge, J. E.: A New Method for the Analysis of Ionospheric h'(f) Records. J. Atmospheric and Terrestrial Phys., vol. 21, no. 1, April 1961, pp. 1-12.

16. Becker, W.: Tables of Ordinary and Extraordinary Refractive Indices, Group Refractive Indices and $h'_{o,x}(f)$ Curves for Standard Ionospheric Layer Models. Max-Plank-Institute für Aeronome, no. 4, 1960, Berlin, Springer.

17. Budden, K. G.: A Method For Determining the Variation of Electron Density With Height [N(z) Curves] From Curves of Equivalent Height Versus Frequency [(h'f) Curves]. Physics of Ionosphere, Phys. Soc. (London), 1955, pp. 332-9.

18. King, G. A. M.: Electron Distribution in the Ionosphere. J. Atmospheric and Terrestrial Phys., vol. 5, no. 4, Sept. 1954, pp. 245-6.

19. Thomas, J. O., and Vickers, M. D.: The Conversion of Ionospheric Virtual Height-Frequency Curves to Electron Density-Height Profiles. DSIR Radio Research Special Rep. 28. Her Majesty's Stationery Office, London, 1959.

20. Doupnik, J. R.: A Flexible Method of Determining the Electron Density Distribution in the Ionosphere. Scientific Ref. 190, Ionosphere Res. Lab., Pennsylvania State Univ., 1963.

21. Unz, H.: A Solution of the Integral Equation, $h'(f) = \int \mu'(f;f_o)dz(f_o)$. J. Atmospheric and Terrestrial Phys., vol. 21, no. 1, Apr. 1961, pp. 40-5.

22. Knecht, R. W., Van Zandt, T. E., and Watts, J. M.: The NASA Fixed Frequency Topside Sounder Program. Paper in "Electron Density Profiles in the Ionosphere and Exosphere," by B. Maehlum, ed., Pergamon Press, 1962, pp. 246-60.

23. Paul, A. K., and Wright, J. W.: Some Results of a New Method For Obtaining Ionospheric N(h) Profiles and Their Bearing on the Structure of the Lower F Region. J. Geophys. Res., vol. 68, no. 19, Oct. 1, 1963, pp. 5413-20.

24. Fitzenreiter, R. J., and Blumle, L. J.: Analysis of Topside Sounder Records. J. Geophys. Res., vol. 69, no. 3, Feb. 1, 1964, pp. 407-13.

25. Jackson, John E.: A New Method For Obtaining Electron-Density Profiles From P'-f Records. J. Geophys. Res., vol. 61, no. 1, March 1956, pp. 107-27.

26. Jackson, J. E.: NASA Investigation of the Topside Ionosphere. NASA X-615-63-105, 1963.

27. Doupnik, J. R., and Schmerling, E. R.: The Reduction of Ionograms From the Bottomside and Topside. Scientific Res. Rep. 230, NASA Grant NsG-134-61, Ionosphere Res. Lab., The Pennsylvania State Univ., Jan 1, 1965.

28. Thomas, J. O.: The Distribution of Electrons in the Ionosphere. Proceedings of the Institute of Radio Engineers, vol. 47, no. 2, Feb. 1959, pp. 162-75.

29. Ratcliffe, J. A.: The Magneto-Ionic Theory and Its Applications to the Ionosphere. Cambridge Univ. Press, 1959.

TABLE I.- TABLE OF REFERENCES. [THE NASA AMES RESEARCH CENTER DIGITAL COMPUTER PROGRAMS FOR h'(f) - N(h) REDUCTION ARE DIRECTLY BASED ON THE TECHNIQUES DESCRIBED IN THE MIDDLE COLUMN]

Method	Direct references	Important related references
Single polynomial	Titheridge, 1961 (ref. 15) Thomas, Long and Westover, 1963 (ref. 13) Thomas and Westover, 1963 (ref. 14)	Unz, 1961 (ref. 21) Knecht, VanZandt and Watts, 1962 (ref. 22)
Overlapping polynomial	Titheridge, 1961 (ref. 15)	
Lamination	Budden, 1954 (ref. 17) King, 1954 (ref. 18) Thomas and Vickers, 1959 (ref. 19)	Paul and Wright, 1963 (ref. 23) Fitzenreiter and Blumle, 1964 (ref. 24) Jackson, 1956, 1963, (refs. 25, 26)
Contiguous parabola	Doupnik, 1963 (ref. 20)	Doupnik and Schmerling, 1965 (ref. 27)
General reviews		Thomas, 1959 (ref. 28)
Appleton-Hartree magneto-ionic theory	Becker, 1960 (ref. 16)	Ratcliffe, 1959 (ref. 29)

TABLE II.- COMPARISON OF EXPONENTIAL MODEL PROFILE AND THE PROFILE DEDUCED FROM THE CORRESPONDING h'(f) CURVE USING THE OVERLAPPING POLYNOMIAL METHOD

h', km	f, Mc/s	Δh, km	
		Computed	Exact
0.0	1.00	0.0	0.0
177.4	1.10	37.5	38.12
248.9	1.20	72.0	72.93
302.6	1.30	103.9	104.94
346.8	1.40	134.0	134.59
385.0	1.50	161.6	162.19
463.5	1.75	223.5	223.85
526.8	2.00	276.9	277.26
626.7	2.50	366.0	366.52
705.1	3.00	439.1	439.44
769.9	3.50	500.6	501.10
825.4	4.00	553.9	554.52
878.9	4.50	602.1	601.63
917.0	5.00	644.2	643.78
955.8	5.50	681.8	681.90
991.2	6.00	716.6	716.70
1024.0	6.50	748.6	748.72
1054.0	7.00	778.3	778.36
1081.0	7.50	805.7	805.96
1107.0	8.00	831.4	831.78

TABLE III.- TOPSIDE WORKING GROUP TEST IONOGRAM

Telemetry station: Singapore
Pass: 697 (19 Nov. 1962)
Frame: 28(0810 UT)

Alouette altitude: 1003.2 km
Subsatellite longitude: 117.2° E
Subsatellite latitude: 11.6° S

f_{Hv} = 0.81 Mc/s; Dip angle = 41°

(h'_o and h'_x are Ordinary and Extraordinary ray virtual depths (km), and f and f_x are Ordinary and Extraordinary ray frequencies of reflection (Mc/s))

Ordinary trace				Extraordinary trace			
h'_o	f	h'_o	f	h'_x	f_x	h'_x	f_x
0	1.63	730	7.50	0	2.08	700	5.50
230	1.70	750	8.00	175	2.10	705	6.00
355	1.80	765	8.50	340	2.20	710	6.50
415	1.90	795	9.00	430	2.30	720	7.00
460	2.00	805	9.10	480	2.40	735	7.50
490	2.10	810	9.20	525	2.50	750	8.00
510	2.20	820	9.30	555	2.60	770	8.50
530	2.30	830	9.40	580	2.70	790	9.00
545	2.40	840	9.50	600	2.80	795	9.10
560	2.50	850	9.60	615	2.90	800	9.20
575	2.60	860	9.70	630	3.00	805	9.30
585	2.70	870	9.80	640	3.10	810	9.40
595	2.80	885	9.90	645	3.20	815	9.50
605	2.90	900	10.00	655	3.30	820	9.60
610	3.00	920	10.10	660	3.40	830	9.70
635	3.50	945	10.20	665	3.50	835	9.80
650	4.00	975	10.30	670	3.60	845	9.90
660	4.50			670	3.70	850	10.00
675	5.00			675	3.80	860	10.10
685	5.50			680	3.90	870	10.20
695	6.00			680	4.00	880	10.30
705	6.50			690	4.50	890	10.40
715	7.00			695	5.00	905	10.50

TABLE IV.- TOPSIDE WORKING GROUP TEST IONOGRAM N(Δh) PROFILE

Δh, km	$N \times 10^{-4}$, cm^{-3}	f_N, Mc/s
0	3.3	1.63
20	3.5	1.68
62	4.0	1.80
100	4.5	1.90
130	5.0	2.00
156	5.5	2.11
180	6.0	2.20
201	6.5	2.29
220	7.0	2.38
237	7.5	2.46
250	8.0	2.54
265	8.5	2.62
279	9.0	2.69
290	9.5	2.77
300	10.0	2.84
378	15.0	3.48
420	20.0	4.01
450	25.0	4.49
473	30.0	4.92
491	35.0	5.31
508	40.0	5.68
519	45.0	6.02
530	50.0	6.35
550	60.0	6.95
568	70.0	7.51
582	80.0	8.03
599	90.0	8.52
611	100.0	8.98
629	110.0	9.42
645	120.0	9.83
667	130.0	10.24

TABLE V.- REDUCTION OF THE TOPSIDE WORKING GROUP TEST IONOGRAM USING THE METHOD OF OVERLAPPING POLYNOMIALS

Ordinary trace			Extraordinary trace			
h', km	f_N, Mc/s	Δh, km	h', km	f_x, Mc/s	f_N, Mc/s	Δh, km
0	1.63	0	0	2.08	1.63	0
230.0	1.70	25.7	175.0	2.10	1.64	9.0
355.0	1.80	62.8	340.0	2.20	1.74	45.1
415.0	1.90	96.7	430.0	2.30	1.84	78.9
460.0	2.00	127.5	480.0	2.40	1.93	111.0
510.0	2.20	180.6	525.0	2.50	2.03	138.3
560.0	2.50	244.4	630.0	3.00	2.51	254.5
610.0	3.00	323.9	665.0	3.50	3.00	329.8
635.0	3.50	380.3	680.0	4.00	3.49	383.9
650.0	4.00	421.7	690.9	4.50	3.99	424.6
660.0	4.50	453.4	695.0	5.00	4.48	456.4
675.0	5.00	479.8	700.0	5.50	4.98	481.9
685.0	5.50	502.3	705.0	6.00	5.48	503.3
695.0	6.00	521.4	710.0	6.50	5.98	521.5
705.0	6.50	538.4	720.0	7.00	6.47	538.0
715.0	7.00	553.7	735.0	7.50	6.97	554.0
730.0	7.50	568.3	750.0	8.00	7.47	569.5
750.0	8.00	583.2	770.0	8.50	7.97	585.0
765.0	8.50	597.5	790.0	9.00	8.46	600.5
795.0	9.00	612.8	800.0	9.20	8.66	606.8
840.0	9.50	631.0	810.0	9.40	8.86	613.2
900.0	10.00	653.0	820.0	9.60	9.06	619.7
			835.0	9.80	9.26	626.5
			850.0	10.00	9.46	633.8

TABLE VI.- REDUCTION OF A NIGHTTIME IONOGRAM USING THE METHOD OF OVERLAPPING POLYNOMIALS

Telemetry Station: Stanford
Pass: 3901 (12 July 1963)
Time: 2256 UT

f_{Hv} = 0.81 Mc/s; Dip angle = 53.78°

h', km	f_x, Mc/s	f_N, Mc/s	Δh, km
0	1.33	0.83	0
468.0	1.36	.86	36.0
725.0	1.40	.89	83.7
971.0	1.43	.91	128.0
1099.0	1.48	.95	193.8
1007.0	1.64	1.09	314.3
876.0	1.89	1.33	401.7
806.0	2.22	1.66	467.3
790.0	2.64	2.08	522.0
803.0	3.13	2.57	569.5
847.0	3.67	3.10	616.2
935.0	4.30	3.75	673.4

TABLE VII.- IONOGRAM DATA INPUT FORMAT FOR N_V PROGRAM

```
PASS    D A T E     T I M E       F X V                       S T A T I O N
        Y R M O D Y H R M N S C
              1 1 1 1 1 1 1 1 1 1 2 2 2 2 2 2 2 2 2 2 3 3 3 3 3 3 3 3 3 3 4 4 4 4 4 4 4 4
1 2 3 4 5 6 7 8 9 0 1 2 3 4 5 6 7 8 9 0 1 2 3 4 5 6 7 8 9 0 1 2 3 4 5 6 7 8 9 0 1 2 3 4 5 6 7
x x x x x x   x x x x x x   x x x x x x       x . x x                           x x x x x x
0 0 3 7 9 4   6 3 0 7 0 4   0 6 1 9 2 3       1 . 7 3                           S T N F R D
```

TABLE VIII.- TABLE DATA INPUT FORMAT FOR N_V PROGRAM

```
P A S S     D A T E     T I M E       L O N G       L A T     H E I G H T *       KP
            Y R M O D Y H R M N S C
              1 1 1 1 1 1 1 1 1 1 2 2 2 2 2 2 2 2 2 2 3 3 3 3 3 3 3 3 3 3 4 4 4 4 4 4 4 4
1 2 3 4 5 6 7 8 9 0 1 2 3 4 5 6 7 8 9 0 1 2 3 4 5 6 7 8 9 0 1 2 3 4 5 6 7 8 9 0 1 2 3 4 5 6 7
x x x x x x   x x x x x x   x x x x x x ± x x x . x x ± x x . x x B O x x x x x x A B B B B A A
  0 3 7 9 4   6 3 0 7 0 4   0 6 1 9 0 0 - 1 1 6 . 7 7   3 5 . 4 9   0 1 0 1 4 2 *           3 0
  0 3 7 9 4   6 3 0 7 0 4   0 6 2 0 0 0 - 1 1 6 . 1 3   3 8 . 8 4   0 1 0 1 5 7 *           3 0
```

TABLE IX.- OUTPUT FORMAT FOR N_V PROGRAM

ALOUETTE TOPSIDE SOUNDER
OBSERVATIONS AT XXXXXX
PASS NUMBER XXXX

```
   U N I V E R S A L                    L O C A L
 D A T E        T I M E        D Y      M O       T I M E      S N L     L O N G
                1 1 1 1 1 1 1 1 1 1 2 2 2 2 2 2 2 2 2 2 3 3 3 3 3 3 3 3 3 4 4 4 4
1 2 3 4 5 6 7 8 9 0 1 2 3 4 5 6 7 8 9 0 1 2 3 4 5 6 7 8 9 0 1 2 3 4 5 6 7 8 9 0 1 2 3
X X X X X X B X X X X X X B B X X B X X X X B X X X X X X B B X B B X X X X X X B B
```

```
                                                                                A N G L E
  L A T       H E I G H T     F X V       F H V           H         D I P
4 4 4 4 4 4 5 5 5 5 5 5 5 5 5 5 6 6 6 6 6 6 6 6 6 7 7 7 7 7 7 7 7 7 8 8 8 8 8 8
4 5 6 7 8 9 0 1 2 3 4 5 6 7 8 9 0 1 2 3 4 5 6 7 8 9 0 1 2 3 4 5 6 7 8 9 0 1 2 3 4 5
X X X X X B B X X X X X X B B X X X X B B X X X X B B X X X X X X B B X X X X X B B
```

```
          L A M B D A     L A M B D A     L                   N         K P
            D I P         I N V H T                         10-5
                                                  1 1 1 1 1 1 1 1 1 1 1 1 1 1 1 1 1
8 8 8 8 9 9 9 9 9 9 9 9 9 0 0 0 0 0 0 0 0 0 0 1 1 1 1 1 1 1 1
6 7 8 9 0 1 2 3 4 5 6 7 8 9 0 1 2 3 4 5 6 7 8 9 0 1 2 3 4 5 6
X X X X X B B X X X X X B B X X X X X X B B X X X X X B B X X
```

TABLE X.- N(h) IDENTIFICATION CARD FORMAT

Column	Item
4-8	Pass number, integer, right adjusted
9-19	Date, any format whatever (e.g., 10 JULY 63, or 7/10/63, etc.)
20-21	Hours } Time
22-23	Minutes } Time
24-25	Seconds } Time

TABLE XI.- N(h) PARAMETER CARD FORMAT

Column	Item
3	Control digit: 0 Ordinary ray data; 1 Extraordinary ray data
4-6	The number of points read from the ionogram, integer, right adjusted
7-12	I_V, dip angle at the position of the satellite, degrees (±XX.XX)
13-18	f_{HV}, gyrofrequency at the position of the satellite, Mc/s (X.XXXX)
19-24	f_V (or f_{XV}), the frequency of the Ordinary ray (or Extraordinary ray) at the position of the satellite, Mc/s (X.XXXX)

TABLE XII.- FREQUENCY-VIRTUAL DEPTH DATA CARDS

Columns	Item	
2-6	f (or f_x), Mc/s	reading i
7-12	h', km	
13-17	f (or f_x), Mc/s	reading i + 1
18-23	h', km	
24-28	f (or f_x), Mc/s	reading i + 2
29-34	h', km	
35-39	f (or f_x), Mc/s	reading i + 3
40-45	h', km	

TABLE XIII.- SPECIAL CONTROL CARD FORMAT[a]

Columns	Item
1-5	The number of points to be computed using the linear lamination method, right adjusted.
6-10	Logical tape upon which the two summary tables are to be written, right adjusted. If this field is blank, or zero, then the table preparation is deleted.

[a]Table XIII is not normally required in routine $h'(f) \rightarrow N(h)$ reduction, the overlapping polynomial method being used with a "three linear lamination" starting procedure.

TABLE XIV.- TYPICAL DETAIL OUTPUT PAGE, OVERLAPPING POLYNOMIAL PROGRAM

ALOUETTE TOPSIDE SOUNDER DATA - NASA AMES RESEARCH CENTER

METHOD OF OVERLAPPING POLYNOMIALS

PASS	DATE	TIME
3759	01JULY 63	172327

DIP ANGLE AT THE VEHICLE = 42.050

ELECTRON GYROFREQUENCY AT THE VEHICLE = 0.7400

EXTRAORDINARY RAY FREQUENCY AT THE VEHICLE = 1.630

EXTRAORDINARY RAY DATA

H PRIME	FX	F PRIME	DELTA H	ELECTRON DENSITY
0.	0.1630E 01	0.1204E 01	0.	0.1797E 05
0.1970E 03	0.1640E 01	0.1213E 01	0.7851E 01	0.1824E 05
0.3520E 03	0.1710E 01	0.1279E 01	0.4236E 02	0.2027E 05
0.5730E 03	0.1790E 01	0.1352E 01	0.9220E 02	0.2265E 05
0.6710E 03	0.1900E 01	0.1454E 01	0.1525E 03	0.2618E 05
0.7410E 03	0.2000E 01	0.1547E 01	0.1990E 03	0.2965E 05
0.8070E 03	0.2230E 01	0.1764E 01	0.2887E 03	0.3856E 05
0.8460E 03	0.2630E 01	0.2150E 01	0.3948E 03	0.5725E 05
0.8560E 03	0.3080E 01	0.2589E 01	0.4756E 03	0.8303E 05
0.8560E 03	0.3580E 01	0.3081E 01	0.5352E 03	0.1176E 06
0.8670E 03	0.4070E 01	0.3566E 01	0.5792E 03	0.1575E 06
0.8950E 03	0.4550E 01	0.4040E 01	0.6172E 03	0.2022E 06
0.9220E 03	0.5050E 01	0.4535E 01	0.6534E 03	0.2548E 06

TABLE XV.- TYPICAL DETAIL OUTPUT PAGE, CONTIGUOUS PARABOLA PROGRAM

TRUE HEIGHT PARABOLIC IN LOG OF PLASMA FREQUENCY

CONTIGUOUS PARABOLA PROGRAM

PASS 3759

DATE 01JULY 63

TIME 172327

DIP ANGLE AT THE VEHICLE = 42.050

ELECTRON GYROFREQUENCY AT THE VEHICLE = 0.7400

EXTRAORDINARY RAY FREQUENCY AT THE VEHICLE = 1.630

F	H	A	B	FN	FH	Z	DELTA H	DENSITY
1.630	0.	9.5363E 02	-3.6946E 03	1.2045	0.7400	1000.00	0.	0.1803E 05
1.640	197.0	9.5363E 02	-3.6946E 03	1.2133	0.7424	992.03	7.97	0.1835E 05
1.710	352.0	4.5859E 02	3.8975E 03	1.2783	0.7544	952.69	47.31	0.2062E 05
1.790	573.0	9.4567E 02	-1.8304E 03	1.3524	0.7682	908.82	91.18	0.2336E 05
1.900	671.0	6.5415E 02	6.0002E 02	1.4531	0.7887	845.12	154.88	0.2740E 05
2.000	741.0	7.3454E 02	-5.2083E 02	1.5465	0.8041	798.61	201.39	0.3132E 05
2.230	807.0	5.9052E 02	-2.5191E 02	1.7633	0.8358	707.00	293.00	0.4130E 05
2.630	846.0	4.8905E 02	-2.6818E 02	2.1481	0.8755	598.30	401.70	0.6179E 05
3.080	856.0	3.8942E 02	-2.0716E 02	2.5871	0.9070	516.70	483.30	0.8959E 05
3.580	856.0	3.1814E 02	-6.5939E 01	3.0793	0.9314	455.84	544.16	0.1264E 06
4.070	867.0	2.9918E 02	7.5557E 01	3.5636	0.9498	411.48	588.52	0.1685E 06
4.550	895.0	3.1778E 02	-2.6343E 01	4.0382	0.9660	373.51	626.49	0.2155E 06
5.050	922.0	3.1179E 02	0.	4.5328	0.9815	337.69	662.31	0.2705E 06

TABLE XVI.- TYPICAL ELECTRON DENSITY SUMMARY TABLE, OVERLAPPING POLYNOMIAL PROGRAM

ALOUETTE TOPSIDE SOUNDER DATA

PASS 3759 DATA 01 JULY 63

ELECTRON DENSITY IN ELECTRONS PER CC (X10-5)

DEPTH	TIME (GMT)								
	171922	172108	172125	172200	172218	172235	172252	172327	172402
0	0.144	0.167	0.160	0.170	0.169	0.171	0.173	0.180	0.195
50	0.177	0.185	0.182	0.193	0.196	0.196	0.198	0.207	0.229
100	0.198	0.208	0.206	0.217	0.222	0.225	0.223	0.231	0.256
150	0.224	0.234	0.233	0.244	0.251	0.251	0.253	0.260	0.290
200	0.257	0.266	0.266	0.275	0.284	0.284	0.287	0.297	0.333
250	0.297	0.306	0.307	0.315	0.325	0.325	0.329	0.344	0.387
300	0.345	0.355	0.357	0.364	0.372	0.376	0.381	0.401	0.453
350	0.410	0.418	0.420	0.432	0.441	0.446	0.450	0.483	0.544
400	0.493	0.504	0.494	0.516	0.527	0.542	0.545	0.586	0.661
450	0.612	0.626	0.615	0.637	0.657	0.658	0.679	0.738	0.824
500	0.782	0.813	0.780	0.824	0.840	0.849	0.885	0.956	1.038
550	1.040	1.088	1.024	1.085	1.130	1.159	1.200	1.297	1.397
600	1.402		1.392	1.530	1.547	1.628	1.671	1.808	2.007
650				1.986	2.079	2.211	2.301	2.495	

TABLE XVII.- TYPICAL SCALE HEIGHT SUMMARY TABLE, OVERLAPPING POLYNOMIAL PROGRAM

ALOUETTE TOPSIDE SOUNDER DATA

PASS 3759 DATA 01 JULY 63

SCALE HEIGHT, KM

DEPTH	TIME (GMT)								
	171922	172108	172125	172200	172218	172235	172252	172327	172402
0									
50									
100	419.3	425.8	400.5	429.4			409.3	432.6	420.5
150	381.7	405.8	387.8	417.2	402.6	424.6	394.7	390.5	379.0
200	353.1	367.9	358.3	386.0	385.4	385.0	374.3	356.4	343.0
250	336.9	342.7	337.0	356.3	370.7	350.6	352.3	330.2	320.4
300	304.5	318.6	317.3	310.9	319.4	311.4	316.5	288.1	288.0
350	276.3	280.9	307.5	283.5	284.3	270.0	274.1	261.3	261.8
400	244.7	241.3	253.5	251.2	244.6	255.2	238.0	229.9	235.9
450	211.9	202.8	215.0	207.4	209.5	214.4	199.4	199.5	218.0
500	182.6	176.1	190.7	184.1	177.6	169.6	169.7	171.0	181.4
550	167.7		167.1	153.6	159.8	148.7	152.8	152.3	144.3
600				169.8	163.1	154.8	151.8	150.9	
650									